

Preliminary in vivo and ex vivo evaluation of the 5-HT_{2A} imaging probe [¹⁸F]MH.MZ

Matthias M. Herth^{a,*}, Markus Piel^a, Fabian Debus^b, Ulrich Schmitt^b,
Hartmut Lüddens^b, Frank Rösch^a

^a*Institute of Nuclear Chemistry Johannes Gutenberg-University Mainz, D-55128 Mainz, Germany*

^b*Department of Psychiatry and Psychotherapy Clinical Research Group, D-55131 Mainz, Germany*

Received 1 January 2009; received in revised form 16 January 2009; accepted 25 January 2009

Abstract

Introduction: The 5-HT_{2A} receptor is one of the most interesting targets within the serotonergic system because it is involved in a number of important physiological processes and diseases.

Methods: [¹⁸F]MH.MZ, a 5-HT_{2A} antagonistic receptor ligand, is labeled by ¹⁸F-fluoroalkylation of the corresponding desmethyl analogue MDL 105725 with 2-[¹⁸F]fluoroethyltosylate ([¹⁸F]FETos). In vitro binding experiments were performed to test selectivity toward a broad spectrum of neuroreceptors by radioligand binding assays. Moreover, first micro-positron emission tomography (μPET) experiments, ex vivo organ biodistribution, blood cell and protein binding and brain metabolism studies of [¹⁸F]MH.MZ were carried out in rats.

Results: [¹⁸F]MH.MZ showed a *K_i* of 3 nM toward the 5-HT_{2A} receptor and no appreciable affinity for a variety of receptors and transporters. Ex vivo biodistribution as well as μPET showed highest brain uptake at ~5 min p.i. and steady state after ~30 min p.i. While [¹⁸F]MH.MZ undergoes extensive first-pass metabolism which significantly reduces its bioavailability, it is insignificantly metabolized within the brain. The binding potential in the rat frontal cortex is 1.45, whereas the cortex to cerebellum ratio was determined to be 2.7 after ~30 min.

Conclusion: Results from μPET measurements of [¹⁸F]MH.MZ are in no way inferior to data known for [¹¹C]MDL 100907 at least in rats. [¹⁸F]MH.MZ appears to be a highly potent and selective serotonergic PET ligand in small animals.

© 2009 Elsevier Inc. All rights reserved.

Keywords: MDL 100907; Altanserin; MH.MZ; PET; Fluorine-18; 5-HT_{2A} receptor

1. Introduction

Serotonin is a neurotransmitter that has been linked to a number of physiological processes and diseases, including appetite, emotion, changes in mood, depression, Alzheimer's disease (AD) and the regulation of the sleep/wake cycle [1,2]. In particular, 5-HT_{2A} receptors have been implicated in the beneficial effects of some antidepressants as well as antipsychotics [3]. Most but not all hallucinogens, including LSD, function as agonists at 5-HT_{2A} receptors, while all clinically approved atypical antipsychotic drugs are potent 5-HT_{2A} receptor antagonists [3].

Therefore, in vivo studies of 5-HT_{2A} receptor occupancy would provide a significant advance in the understanding of the mentioned disorders and conditions.

Positron emission tomography (PET) is an appropriate tool to measure in vivo directly, noninvasively and repetitively the binding potential (BP), the receptor availability and uptake kinetics of radio tracers for neuroreceptors.

Successful radioligands studied in in vivo PET investigations to date for molecular imaging of the 5-HT_{2A} system are antagonistic ligands such as [¹¹C]MDL 100907 [4–6] and [¹⁸F]altanserin [7–10]. It could be demonstrated that patients with mild cognitive impairment show a reduced 5-HT_{2A} receptor binding [9]. Furthermore, there is substantial evidence from recent PET studies in humans to implicate dysfunction of the serotonergic transmitter system in the AD [10]. For example, in vivo functional imaging studies have

* Corresponding author. Tel.: +49 6131 39 25849; fax: +49 6131 39 24692.

E-mail address: herthm@uni-mainz.de (M.M. Herth).

confirmed large reductions in 5-HT_{2A} receptor binding in mild to moderately demented AD patients using PET [11,12]. Moreover, the implication of the 5-HT_{2A} receptor in the AD has also been reported by consistent postmortem findings. A reduction in the availability of the 5-HT_{2A} receptor subtype could be determined [13–16].

Currently, [¹⁸F]altanserin and [¹¹C]MDL 100907 are the most frequently used PET tracers to probe for the 5-HT_{2A} receptor in vivo due to their high affinity and selectivity for the 5-HT_{2A} receptor (altanserin: $K_i=0.13$ nM [7]; (R)-MDL 100907: $K_i=0.2$ nM [4]). Binding to other 5-HT receptor subtypes is very low for [¹¹C]MDL 100907 [17] and moderate to low for [¹⁸F]altanserin [18]. A further difference between these two tracers is their binding to receptors other than the serotonergic system. Altanserin shows a relatively high affinity for D₂ receptors (62 nM) and adrenergic- α_1 receptors (4.55 nM) [18], whereas the BP of MDL 100907 to these receptors is insignificant [19]. Another drawback of [¹⁸F]altanserin is its rapid and extensive metabolism [18]. A disadvantage of [¹¹C]MDL 100907 is its slow kinetics combined with the short half-life of the β^+ -emitter ¹¹C. The main advantage of [¹⁸F]altanserin over [¹¹C]MDL 100907 is the possibility to perform equilibrium scans lasting several hours and to transport the tracer to other facilities based on the 110 min half-life of ¹⁸F-fluorine.

In summary, [¹¹C]MDL 100907 is a very specific high-affinity ligand for 5-HT_{2A} receptors with the disadvantages of the short half-life of C-11 and its slow kinetics [6]. The binding of [¹⁸F]altanserin lacks specificity and in vivo stability, but due to its availability, it is the most commonly used receptor ligand for 5-HT_{2A} imaging.

Consequently, recent attempts were tried to synthesize [¹⁸F]MDL 100907 [20]. However, due to the very low radiochemical yield of 2%, this ligand is not suitable for in vivo studies. In contrast, we have reported the synthesis (Fig. 1) [21], first in vitro and ex vivo evaluation studies of an ¹⁸F-analog of MDL 100907, [¹⁸F]MH.MZ (1), to create a ligand combining the better selectivity of MDL 100907 as compared to altanserin and the superior isotopic properties of ¹⁸F-fluorine as compared to ¹¹C-carbon (concerning both half-life and spatial resolution of PET measurements). Thereby, the affinity of MH.MZ toward the 5-HT_{2A} receptor was determined to be $K_i=3.00\pm 0.10$ nM and thus 15 times lower than that of the parent compound MDL 100907 ($K_i=0.2$ nM) [4]. Overall labeling yields are 30–50%. These results indicate an improved clinical applica-

tion profile and justified further examination of the potential of [¹⁸F]MH.MZ for molecular imaging the 5-HT_{2A} receptor.

2. Methods and materials

2.1. Chemicals and reagents

Chemicals were purchased from Acros, Fluka or Merck. Unless otherwise noted, all chemicals were used without further purification.

2.2. Synthesis of the precursor MDL 105725 of [¹⁸F]MH.MZ

MDL 105725 was synthesized as reported by Ullrich et al. [22].

2.3. Production of [¹⁸F]MH.MZ

2.3.1. [¹⁸F]FETos synthon synthesis

Kryptofix 222 (10 mg, 25 mmol), 12.5 ml potassium carbonate (1 N) and 1 ml acetonitrile were added to an aqueous [¹⁸F]fluoride solution (1400–1600 MBq). The mixture was dried in a stream of nitrogen at 80°C. The drying procedure was repeated three times until the reaction mixture was absolutely dry. The dried Kryptofix 222/[¹⁸F]fluoride complex was then dissolved in 1 ml acetonitrile, and 4 mg (10 mmol) ethylene glycol-1,2-ditosylate was added and heated under stirring in a sealed vial for 3 min. Purification of the crude product was accomplished using HPLC (Lichrospher RP18-EC5, 250×10 mm; acetonitrile/water 50:50, flow rate: 5 ml/min, rt: 8 min). After diluting the HPLC fraction containing the 2-[¹⁸F]fluoroethyltosylate with water, the product was loaded on a Phenomenex strata-X 33- μ m polymeric reversed-phase column, dried with nitrogen and eluted with 1 ml of tempered (40–50°C) DMSO.

2.3.2. Radiolabeling

[¹⁸F]FETos diluted in 0.8 ml of dry DMSO was added to a solution of 3 mg MDL 105725 (7 mmol) dissolved in 0.2 ml dry DMSO and 1.5 μ L 5N NaOH (7 mmol). The solution remained at 100°C for 10 min and was quenched with 1 ml H₂O. Reactants and by-products were separated from [¹⁸F]MH.MZ by semipreparative HPLC [μ Bondapak C₁₈ 7.8×300 mm column, flow rate 8 ml/min, eluent: MeCN/0.05 phosphate buffer pH 7.4 adjusted with H₃PO₄ (40:60)].

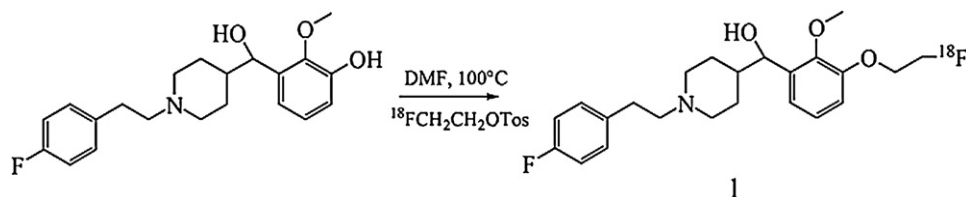


Fig. 1. Radiosynthesis of [¹⁸F]MH.MZ.

The retention times of [^{18}F]MH.MZ, [^{18}F]FETos and MDL 105725 were 9.8, 4.0 and 4.9 min, respectively. The collected product was diluted with water (4:1), passed through a conditioned strata-X cartridge (1 ml EtOH, 1 ml H_2O), washed with 10 ml H_2O and eluted with at least 1 ml EtOH. Finally, EtOH was removed in vacuo and [^{18}F]MH.MZ dissolved in 1 ml saline.

2.3.3. Determination of radiochemical purity and specific activity

The radiotracer preparation was visually inspected for clarity, absence of color and particulates. Chemical and radiochemical purities were also assessed by TLC analyses and by analytical LUNA 250 \times 4.6 mm 5 C_{18} (2); eluent: MeCN/buffer (0.05 M Na_2HPO_4 adjusted to pH=6.7 with H_3PO_4), RT: [^{18}F]F $^-$ =2.4 min; [^{18}F]FETos=22.0 min; [^{18}F]MH.MZ=11.3 min; MDL 105725=4.8 min; flow rate 1 ml/min; SiO_2 -TLC: eluent: $\text{CHCl}_3/\text{MeOH}/\text{conc. NH}_3$ 8:1:0.2, R_f [^{18}F]MH.MZ: 0.36, [^{18}F]FETos: 0.95 and R_f [^{18}F]fluoride ion: 0.0). Specific activity (A_s) of the radiotracer was calculated from three consecutive HPLC analyses (average) and determined as follows: the area of the UV absorbance peak corresponding to the radiolabeled product was measured (integrated) on the HPLC chromatogram and compared to a standard curve relating mass to UV absorbance.

2.4. Animals

Male 8-week mature catheterized Sprague–Dawley rats were obtained from Charles River Laboratories, France. In addition, Wistar rats obtained from the animal husbandry of the Johannes Gutenberg University of Mainz were used for ex vivo distribution studies. All procedures were carried out in accordance with the European Communities Council Directive regarding care and use of animals for experimental procedures and were approved by local authorities of the state of Rheinland-Pfalz.

2.5. Binding assays

Binding assays were performed by the National Institute of Mental Health's Psychoactive Drug Screening Program (NIMH PDSP) at the Department of Biochemistry, Case Western Reserve University, Cleveland, OH, USA (Bryan Roth, Director). Compound (1) was assayed for its affinities for a broad spectrum of receptors and transporters in competitive binding experiments in vitro using cloned human receptors. Reported values of the inhibition coefficient (K_i) are mean \pm S.D. of four separate determinations.

2.6. Ex vivo organ biodistribution

Fully grown male Wistar rats (weight 250–310 g) were injected with ~ 10 MBq of [^{18}F]MH.MZ via tail vein. At 5, 15, 30 and 60 min post injection, animals were euthanized, and blood and the indicated tissues removed. The radioactivity in brain, kidneys, liver, stomach and bones was

determined. Data were corrected for decay and reported as mean percentage of the injected dose per gram of tissue (% ID/g tissue).

2.7. [^{18}F]MH.MZ metabolism studies in the brain

At 60 min p.i., Wistar rats (weight 250–310 g) were anesthetized with halothane and sacrificed. Blood samples for determination of the metabolism were centrifuged, and the supernatant was mixed with MeCN 1:5. After an additional centrifugation step, the supernatant was used for chromatography (radio-TLC). Brains for determination of the metabolism were harvested, homogenized and mixed with MeOH and centrifuged. The supernatant was used for TLC. Blood and brain samples were analyzed via TLC ($\text{CHCl}_3/\text{MeOH}$ 5:2; R_f [^{18}F]FETos: 0.9, [^{18}F]MH.MZ: 0.7 and metabolite 0.1).

2.8. Blood cell and protein binding of [^{18}F]MH.MZ

The ratio of radioactivity concentration in blood cells vs. protein and plasma water was determined in three Wistar rats. Four blood samples were obtained from 0 to 60 min (5, 10, 30 and 60 min, respectively) after intravenous injection of [^{18}F]MH.MZ. Whole blood was centrifuged at 10,000 rpm for 5 min at 4°C to separate plasma and blood cells. Plasma and blood cell fractions were obtained, and the radioactivity was measured with an automatic γ -counter (2470 Wizard²; Perkin Elmer). Subsequently, plasma proteins were precipitated with MeCN (1:4), centrifuged at 10,000 rpm for 10 min at RT, and the radioactivity in supernatant (plasma water) and sediment was measured using the mentioned γ -counter. The percentage of radioactivity bound to plasma proteins was calculated thereafter.

2.9. μPET experiments

μPET imaging was performed with a Siemens/Concorde Microsystems microPET Focus 120 small animal PET camera. Animals were 250 g, 8-week-old Sprague–Dawley rats bought with catheters in the femoral artery and vein. Animals were anesthetized with volatile anesthetic isoflurane at a concentration of 1.8%. The radiotracer was applied via intravenous injection into the femoral vein catheter (~ 10 MBq, $A_s=50$ GBq/ μmol), and blood samples were collected via the femoral artery catheter. After application of [^{18}F]MH.MZ or collecting of blood samples, catheters were flushed with heparinized isotonic 0.9% NaCl solution. Volumes of blood collected were reinjected as isotonic 0.9% NaCl solution. Results were expressed as standardized uptake values (SUVs), which is defined by (activity concentration in becquerel per milliliter)*(body weight in gram)/(injected dose in becquerel). Scans were carried out as dynamic scans over a time period of 60 min. Kinetic modeling and image quantification were done using the PMOD software package and a four-parameter reference tissue model.

3. Results and discussion

As previously reported, [^{18}F]MH.MZ could be obtained as an injectable solution in radiochemical yields of about 42% within a synthesis time of about 100 min in a purity of >96% [21]. Thereby, high specific activities of ~ 50 GBq/ μmol with a batch activity of ~ 3 GBq were obtained.

The capability of the tracer related to its affinity and selectivity was examined by determining binding affinities (K_i) to a broad spectrum of receptors by radioligand binding assays through the NIMH PDSP. Results are summarized in Table 1. The new compound (1) has an excellent K_i of 3.0 nM for the 5-HT $_{2A}$ receptor. In contrast, K_i values for the other receptors and transporters are negligible (Table 1).

Ex vivo organ biodistribution of [^{18}F]MH.MZ was carried out in Wistar rats. Three adult male rats were used for each of four time points. Each animal was injected via tail vein. At 5, 15, 30 and 60 min post injection, animals were euthanized, and blood and the indicated tissues removed. The radioactivity in brain, kidneys, liver, stomach and bones was determined. Data were corrected for decay and reported as mean % ID/g tissue (Table 2). [^{18}F]MH.MZ showed highest brain uptake ($0.48\pm 0.16\%$ ID/g tissue) at 5 min p.i. and steady state appeared to be between ~ 30 and 60 min post injection (Fig. 2). The highest % ID/g tissue could be detected in metabolizing tissues. Maximum accumulation occurred in the liver at 5 min post injection, whereas the maximum accumulation in the kidneys was reached at ~ 15 min post injection. Blood showed highest uptake 15 min p.i., and even after 60 min, steady state is not reached. According to Bonaventure et al. [23], the 5-HT $_{2A}$ receptor concentration in the spleen, the stomach, the testis, the colon and the smooth muscle is about the same level at least in dogs.

Table 1
In vitro binding affinities of MH.MZ toward human receptors and transporters

Target K_i (nM)	Target K_i (nM)
5-HT $_{1A}$	>10.000
5-HT $_{1B}$	1846 \pm 426
5-HT $_{1E}$	>10.000
5-HT $_{2A}$	3 \pm 0
5-HT $_{2B}$	299 \pm 27
5-HT $_{2C}$	71 \pm 10
5-HT $_3$	>10.000
5-HT $_{5A}$	>10.000
5-HT $_6$	3890 \pm 1921
5-HT $_7$	116 \pm 14
KOR	>10.000
M1	>10.000
M3	>10.000
M5	>10.000

Affinities were determined by PDSP. 5-HT, serotonin; SERT, serotonin transporter; D, dopamine; DAT, dopamine transporter; DOR, delta opioid receptors; H, histamine; KOR, kappa opioid receptors; M, muscarinic; MOR, opioid receptor μ -splice variant.

Table 2
Organ biodistribution of [^{18}F]MH.MZ in male SD rats

Tissue	5 min	15 min	30 min	60 min
Brain	0.48 \pm 0.16	0.17 \pm 0.03	0.08 \pm 0.01	0.08 \pm 0.01
Blood	2.39 \pm 0.90	1.37 \pm 0.24	0.69 \pm 0.12	0.33 \pm 0.05
Bones	0.08 \pm 0.04	0.04 \pm 0.02	0.05 \pm 0.01	0.06 \pm 0.01
Stomach	0.32 \pm 0.12	0.44 \pm 0.16	0.37 \pm 0.05	0.34 \pm 0.08
Kidneys	2.74 \pm 0.41	4.31 \pm 2.40	3.64 \pm 1.76	1.76 \pm 0.61
Liver	5.52 \pm 0.94	4.31 \pm 0.50	2.98 \pm 0.28	1.62 \pm 0.29

Radioactivity concentrations are expressed as percentage of the injected dose per gram of tissue (% ID/g tissue). Results are expressed as mean \pm S.D. ($n=3$).

Therefore, we decided to harvest only the stomach. As no significant accumulation in the stomach could be detected, any additional tissues were harvested.

For the analysis of preliminary in vivo metabolism of [^{18}F]MH.MZ in brain and blood, samples were treated as described. Metabolite and intact tracer were analyzed by radio-TLC ($\text{CHCl}_3/\text{MeOH}$ 5:2). The tracer underwent fast metabolism [21]. Only one polar metabolite was found in plasma, and the percentage of unmetabolized fractions was 43%, 32%, 16% and 7% at 5, 10, 30 and 60 min, respectively.

In contrast, Fig. 3 compares metabolized fractions of [^{18}F]MH.MZ in rat plasma and rat brain at 60 min post injection. Radio-TLC analyses showed nonmetabolized [^{18}F]MH.MZ in rat brain samples, whereas almost no intact [^{18}F]MH.MZ could be found in rat plasma.

Probably, the fluoroethoxy group is metabolized similar to the already published behavior of the metabolism of [^{11}C]MDL 100907 [24]. The observed radioactive polar metabolite in Fig. 3 may not cross the blood–brain barrier (BBB) to a large extent because of its polarity. Therefore, we expect that the radioactive metabolite is not able to interfere with the μPET imaging. In addition, our reported time–activity curves (TACs) confirm this hypothesis. No additional accumulation could be observed in the brain after 500 s,

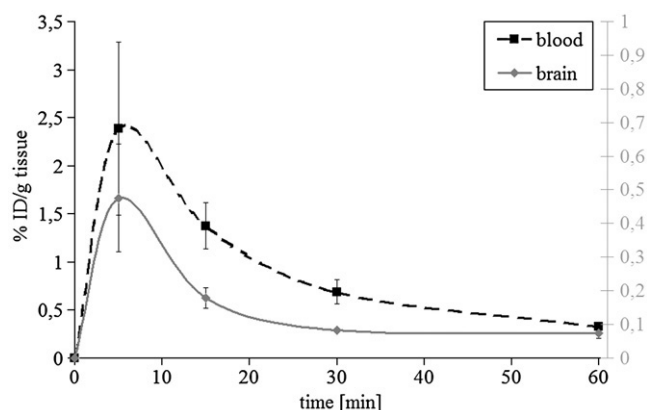


Fig. 2. Ex vivo biodistribution of [^{18}F]MH.MZ in rat brain and blood at 5, 15, 30 and 60 min ($n=3$ per time point; means \pm S.D. shown) following tail vein injection. Results are expressed as % ID/g tissue.

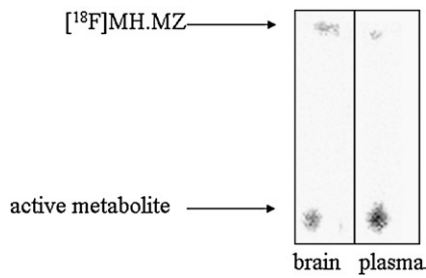


Fig. 3. Comparison of metabolism in rat brain and plasma 60 min post injection. Unmetabolized tracer could be found in rat brain (A), whereas almost no intact tracer could be detected in plasma samples (B).

whereas the metabolite concentration still rises in the blood (Fig. 4). Therefore, we believe that the metabolite found is based on blood still located in vessels in the brain rather than beyond the BBB. However, this is mainly based on assumptions and it could very well be that the active metabolite is within the brain. This would be a considerable drawback of this tracer. Future studies will be carried out to identify this metabolite, its biochemical behavior and its possibility to enter the brain to prove usefulness as a human PET 5-HT_{2A} tracer.

Moreover, protein binding and distribution of [¹⁸F]MH.MZ in rat blood were determined. After intravenous injection of [¹⁸F]MH.MZ into the study subjects (n=4), free tracer is rapidly metabolized as previously reported [21]. The plasma-to-blood ratio of radioactivity was determined to be ~0.65 after 5–10 min and changed over 60 min to a value of ~0.85. This is exactly the time frame used for PET imaging of

[¹⁸F]MH.MZ in this manuscript. Approximately 40% of [¹⁸F]MH.MZ was bound to rat plasma proteins after 60 min, whereas only ~25% was bound after 10 min. The radioactivity bound to blood cells decreases over 60 min from about 30% to 25%. Fig. 4 summarizes the radioactivity distribution in rat blood cells during a 60 min time frame.

First μPET experiments (n=4) were performed with a Siemens MicroPET Focus 120 camera in male 8-week mature catheterized Sprague–Dawley rats. Rats were anesthetized with isoflurane. The binding of [¹⁸F]MH.MZ is displayed in transversal (A), in sagittal (B) and in coronal orientation (C) in Fig. 5. Images are displayed in false color coding with white representing maximum and black representing minimum binding.

Images displayed in Fig. 5 represent summed images of a period of the last 20 min of the scan time. Highest specific uptake is visible in the frontal cortex. High nonspecific uptake was detected in the Harderian glands and in the salivary and thyroid glands. Binding of [¹⁸F]MH.MZ in the cerebellum is at background level. Thus, images represent a visualization of the system in equilibrium binding.

This in vivo distribution is in very good agreement with the distribution recently shown in the autoradiographic images (Fig. 6) [21].

Fig. 7 shows a representative TAC of a total binding study of [¹⁸F]MH.MZ which included four animals. Results are given as SUV.

Equilibrium appears to be reached between 28 to 35 min post injection. The fact that the equilibrium state seems to be reached earlier than observed by Lundkvist et al. [25] is not too surprising given the faster metabolism of rodents as

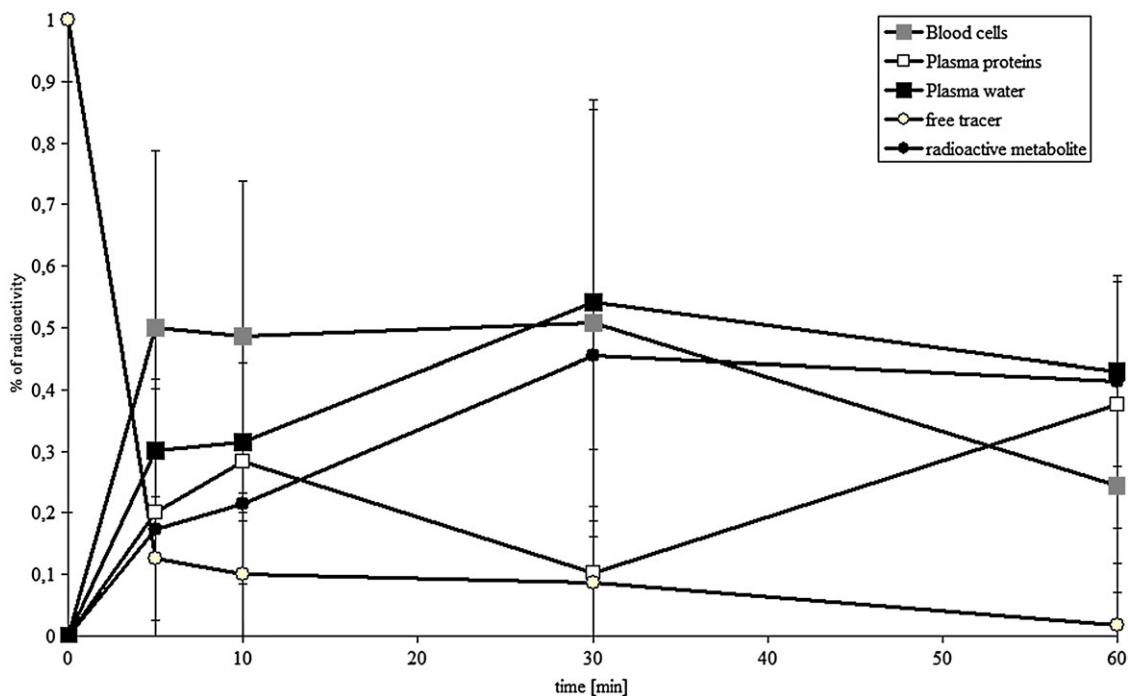


Fig. 4. Distribution of radioactivity derived from [¹⁸F]MH.MZ in rat blood components.

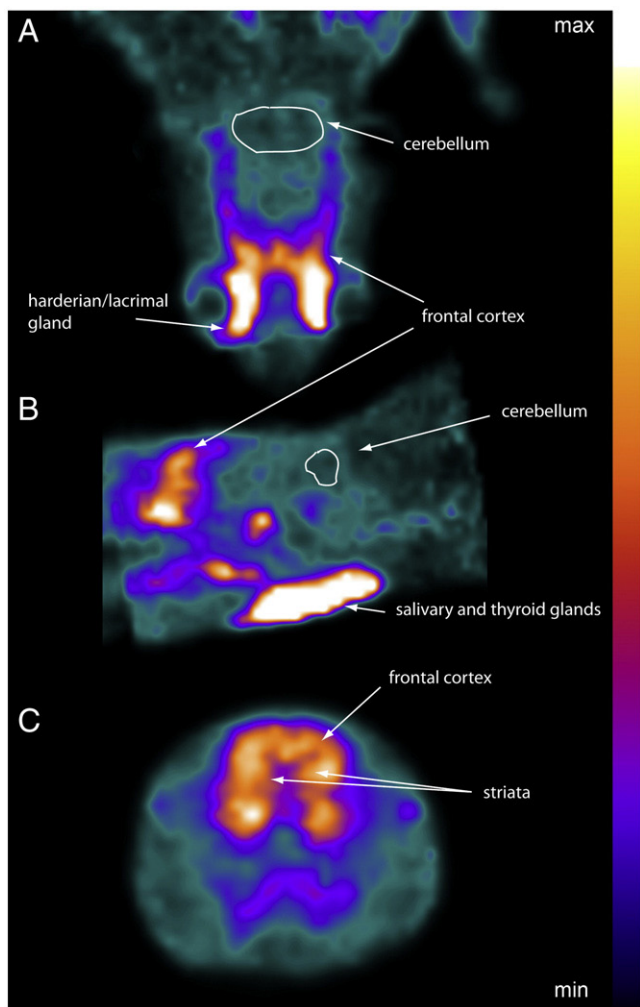


Fig. 5. μ PET images of $[^{18}\text{F}]\text{MH.MZ}$ with (A) transversal, (B) sagittal and (C) coronal orientation.

compared to primates. Once equilibrium binding is reached, the specific binding remains very constant and might therefore even enable scans up to 2 h.

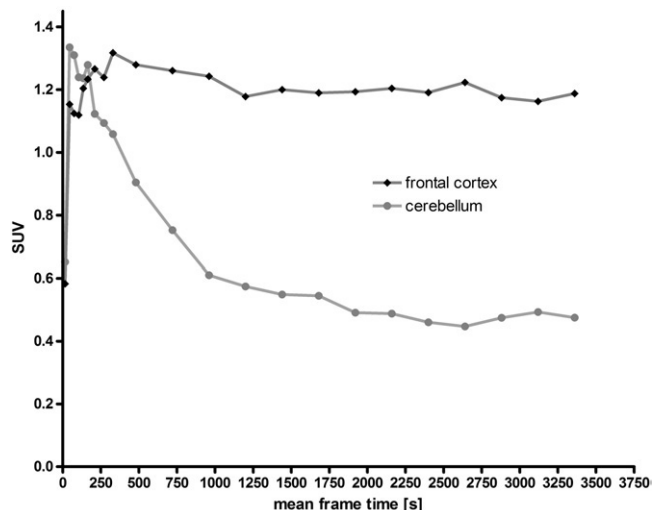


Fig. 7. TAC of μ PET experiments with $[^{18}\text{F}]\text{MH.MZ}$ in SD rats. The graphs show results of a total binding study.

Uptake of $[^{18}\text{F}]\text{MH.MZ}$ in near equilibrium state ($t > 2000$ s) is more than 50% higher in cortical regions than in the cerebellum. The cortex-to-cerebellum ratio was determined to be 2.7 after ~ 40 min ($n=4$), which surprisingly resembles the primate ratios published by Lundkvist et al. [25] measured by $[^{11}\text{C}]\text{MDL 100907}$. This is much likely due to the decreased affinity of MH.MZ compared to MDL 100907. The BP was 1.45 ($n=4$) for the frontal cortex region using a four-parameter reference tissue model and the PMOD software. Cerebellum uptake is employed instead of a plasma input curve.

4. Conclusion

In conclusion, $[^{18}\text{F}]\text{MH.MZ}$ appears to be a suitable new PET tracer for molecular imaging of the 5-HT_{2A} receptor

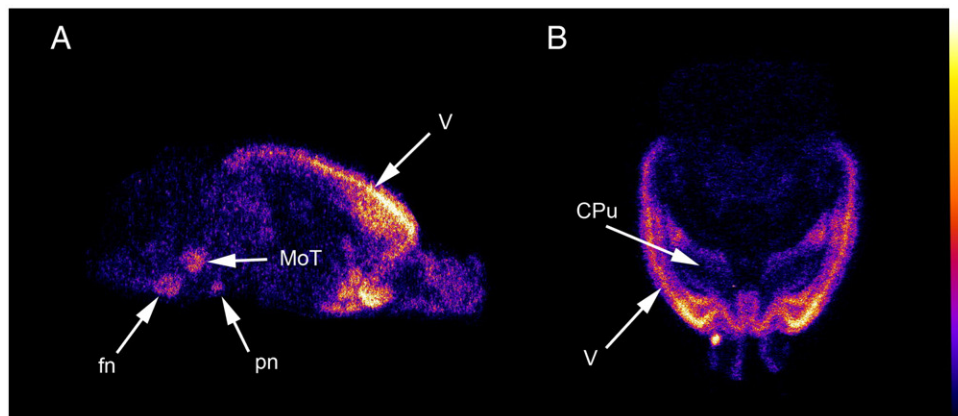


Fig. 6. Images of an autoradiography of $[^{18}\text{F}]\text{MH.MZ}$ binding at 14- μm -thick rat brain sections. (A and B) Total binding at a concentration of 5 nM with (A) lateral 0.9 mm and (B) coronal 5.8 mm from bregma. Major binding was detected in lamina V (V) of the frontal cortex, in caudate-putamen (CPu) and in three regions of the brain stem, the motor trigeminal nucleus (MoT), the facial nucleus (fn) and the pontine nuclei (pn).

system. It offers high affinity ($K_i=3$ nM) for the 5-HT_{2A} receptor and has any appreciable affinity for most of the tested receptors and transporters (Table 1) thus representing excellent specificity. However, the affinity is 15 times lower than that of its parent MDL 100907. For rats, ex vivo biodistribution study as well as μ PET data showed highest brain uptake at ~ 5 min p.i. Equilibrium is reached at ~ 30 min post injection and stays on almost the same level for a relatively long time of about 1 h.

Nonmetabolized [¹⁸F]MH.MZ is present in rat brain samples in contrast to rat plasma after 60 min, indicating that [¹⁸F]MH.MZ is able to cross the BBB whereas metabolites were probably not accumulating in the brain. However, this has to be checked in more detail. For example, the metabolite and its biochemical behavior should be identified, especially if the metabolite is able to cross the BBB. The characteristics observed for [¹⁸F]MH.MZ meet the requirements for molecular imaging and quantitative data interpretation and might be evidently an improvement compared to [¹⁸F]altanserin and be particularly relevant as [¹⁸F]altanserin undergoes rapid and extensive metabolism forming ¹⁸F-containing metabolites that cross the BBB. Results from small animal PET measurements of [¹⁸F]MH.MZ are in no way inferior to data obtained with [¹¹C]MDL 100907. High uptake can be seen in the same brain regions. The BP of [¹⁸F]MH.MZ for uptake in the rat frontal cortex is defined to be 1.45, whereas the cortex-to-cerebellum ratio was determined to be 2.7 at equilibrium ($n=4$). Nevertheless, the usefulness of [¹⁸F]MH.MZ has to be tested in the primate brain because ratios may decrease by going from rat to primate brains.

All together, new auspicious results concerning the biological behavior of [¹⁸F]MH.MZ by both in vivo and ex vivo experiments are reported. Compared to known tracers, the data hint on a considerably improved 5-HT_{2A} imaging ligand at least in rats. Whether [¹⁸F]MH.MZ is an improvement to the already used 5-HT_{2A} tracers in primates is dependent on the possibility of the metabolite to enter the brain. A toxicology study is planned, and provided that it will result in a nontoxicity of the tracer, first human PET studies in healthy volunteers would be possible. Moreover, the polar metabolite will be determined and investigated in more detail.

Acknowledgments

The authors wish to thank Sabine Höhnemann and Vasko Kramer for the syntheses of [¹⁸F]FETos. They also thank Daniel Zils for technical assistance and excellent animal preparation as well as Matthias Schreckenberger, MD, for his support. Financial support by Friedrich-Naumann-Stiftung, the European Network of Excellence (EMIL) is gratefully acknowledged. K_i determinations were generously provided by the NIMH PDSP (Contract No. NO1MH32004). The NIMH PDSP is directed by Bryan L. Roth, MD, PhD, from the University of North Carolina at

Chapel Hill and Project Officer Jamie Driscoll at NIMH, Bethesda MD, USA.

References

- [1] Davis KL, Charney D, Coyle JT, Nemeroff C. Neuropsychopharmacology: the fifth generation of progress. New York: Raven Press; 2002.
- [2] Jones BE, Kryger MH, Roth T, Dement WC, editors. Principles and practice of sleep medicine. Philadelphia: W.B. Saunders Company; 2000. p. 134–54.
- [3] Meltzer HY, Matsubara S, Lee JC. Classification of typical and atypical antipsychotic drugs on the basis of dopamine D-1, D-2 and serotonin2 pKi values. *J Pharmacol Exp Ther* 1989;251:238–46.
- [4] Ito H, Nyberg S, Halldin C, Lundkvist C, Farde L. PET imaging of central 5-HT_{2A} receptors with carbon-11-MDL 100,907. *J Nucl Med* 1998;39:208–14.
- [5] Bhagwagar Z, Hinz R, Taylor M, Fancy S, Cowen P, Grasby P. Increased 5-HT_{2A} receptor binding in euthymic, medication-free patients recovered from depression: a positron emission study with [¹¹C]MDL 100,907. *Am J Psychiatry* 2006;163:1580–7.
- [6] Watabe H, Channing MA, Der MG, Adams RH, Jagoda E, Herscovitch P, et al. Kinetic analysis of the 5-HT_{2A} ligand [¹¹C]MDL 100,907. *J Cereb Blood Flow Metab* 2000;20:899–909.
- [7] Smith GS, Price JC, Lopresti BJ, Huang Y, Simpson N, Holt D, et al. Test–retest variability of serotonin 5-HT_{2A} receptor binding measured with positron emission tomography and [¹⁸F]altanserin in the human brain. *Synapse* 1998;30:380–92.
- [8] Pinborg LH, Arfan H, Haugbol S, Kyvik KO, Hjelmborg J, Svarer C, et al. The 5-HT_{2A} receptor binding pattern in the human brain is instead genetically determined. *Neuroimage* 2008;40:1175–80.
- [9] Hasselbalch SG, Madsen K, Svarer C, Pinborg LH, Holm S, Paulson OB, et al. Reduced 5-HT_{2A} receptor binding in patients with mild cognitive impairment. *Neurobiol Aging* 2008;29:1830–8.
- [10] Meltzer CC, Smith G, DeKosky ST, Pollock BG, Mathis CA, Moore RY, et al. Serotonin in aging, late-life depression, and Alzheimer's disease: the emerging role of functional imaging. *Neuropsychopharmacology* 1998;18:407–30.
- [11] Meltzer CC, Price JC, Mathis CA, Greer PJ, Cantwell MN, Houck PR, et al. PET imaging of serotonin type 2A receptors in late-life neuropsychiatric disorders. *Am J Psychiatry* 1999;156:1871–8.
- [12] Blin J, Baron JC, Dubois B, Crouzel C, Fiorelli M, Attar-Levy D, et al. Loss of brain 5-HT₂ receptors in Alzheimer's disease. In vivo assessment with positron emission tomography and [¹⁸F]setoperone. *Brain* 1993;116:497–510.
- [13] Bowen DM, Najlerahim A, Procter AW, Francis PT, Murphy E. Circumscribed changes of the cerebral cortex in neuropsychiatric disorders of later life. *Proc Natl Acad Sci* 1989;86:9504–8.
- [14] Cheng AV, Ferrier IN, Morris CM, Jabeen S, Sahgal A, McKeith IG, et al. Cortical serotonin-S2 receptor binding in Lewy body dementia. Alzheimer's and Parkinson's diseases. *J Neurol Sci* 1991;106:50–5.
- [15] Lai MK, Tsang SW, Alder JT, Keene J, Hope T, Esiri MM, et al. Loss of serotonin 5-HT_{2A} receptors in the postmortem temporal cortex correlates with rate of cognitive decline in Alzheimer's disease. *Psychopharmacology* 2005;179:673–7.
- [16] Reynolds GP, Arnold L, Rossor MN, Iversen LL, Mountjoy CQ, Roth M. Reduced binding of ketanserin to cortical 5-HT₂ receptors in senile dementia of the Alzheimer type. *Neurosci Lett* 1984;44:47–51.
- [17] Johnson MP, Siegel BW, Carr AA. [³H]MDL 100,907: a novel selective 5-HT_{2A} receptor ligand. *Naunyn Schmiedeberg's Arch Pharmacol* 1996;354:205–9.
- [18] Tan P, Baldwin RM, Fu T, Charney DS, Innis RB. Rapid synthesis of F-18 and H-dual labeled altanserin, a metabolically resistant PET ligand for 5-HT_{2A} receptor. *J Labelled Compd Radiopharm* 1999;42:457–67.
- [19] Hall H, Farde L, Halldin C, Lundkvist C, Sedvall G. Autoradiographic localization of 5-HT_{2A} receptors in the human brain using [³H]M100907 and [¹¹C]M100907. *Synapse* 2000;38:421–31.

- [20] Mühlhausen U, Ermert J, Herth MM, Coenen HH. Synthesis, radiofluorination and first evaluation of (\pm)-[^{18}F]MDL 100907 as serotonin 5-HT_{2A} receptor antagonist for PET. *J Labelled Compd Radiopharm* 2008;52:6–12.
- [21] Herth MM, Debus F, Piel M, Palner M, Knudsen GM, Lüddens H, et al. Total synthesis and evaluation of [^{18}F]MH.MZ. *Bioorg Med Chem Lett* 2008;18:1515–9.
- [22] Ullrich T, Ice KC. A practical synthesis of the serotonin 5-HT_{2A} receptor antagonist MDL 100907, its enantiomer and their 3-phenolic derivatives as precursors for [^{11}C]labeled PET ligands. *Bioorg Med Chem* 2000;8:2427–32.
- [23] Bonaventure P, Nepomuceno D, Miller K, Chen J, Kuei C, Kamme F, et al. Molecular and pharmacological characterization of serotonin 5-HT_{2A} and 5-HT_{2B} receptor subtypes in dog. *Eur J Pharmacol* 2005; 513:181–92.
- [24] Scott DO, Heath TG. Investigation of the CNS penetration of a potent 5-HT_{2A} receptor antagonist (MDL 100,907) and an active metabolite (MDL 105,725) using in vivo microdialysis sampling in the rat. *J Pharm Biomed Anal* 1998;17:17–25.
- [25] Lundkvist C, Halldin C, Ginovart N, Nyberg S, Swahn CG, Carr AA, et al. [^{11}C]MDL 100907, a radioligand for selective imaging of 5-HT_{2A} receptors with positron emission tomography. *Life Sci* 1996;58:187–92.